

Data reduction for XAS experiments with the 100 element Ge Detector

This content has been downloaded from IOPscience. Please scroll down to see the full text.

2016 J. Phys.: Conf. Ser. 712 012016

(<http://iopscience.iop.org/1742-6596/712/1/012016>)

View [the table of contents for this issue](#), or go to the [journal homepage](#) for more

Download details:

IP Address: 131.169.95.162

This content was downloaded on 01/12/2016 at 14:59

Please note that [terms and conditions apply](#).

You may also be interested in:

[METHODS IN DATA REDUCTION: 1. ANOTHER LOOK AT LEAST SQUARES](#)

Deane M. Peterson

[ERRATUM - METHODS IN DATA REDUCTION - PART ONE - ANOTHER LOOK AT LEAST SQUARES](#)

D. M. Peterson

[Pressure induced phase transitions in amorphous Ge](#)

E Principi, F Decremps, A Di Cicco et al.

[EasyLife System for VIPERS](#)

B. Garilli, L. Païoro, M. Scodreggio et al.

[PES and XAS studies of double perovskite oxides: Ba₂xLaxFeMoO₆](#)

J-S Kang, S C Wi, S S Lee et al.

[Structural and morphological characterization of Mo coatings for high gradient accelerating structures](#)

Y Xu, B Spataro, S Sarti et al.

[A Combined Conductivity and XAS Study of Plastically Crystalline Electrolytes](#)

A V Chadwick, A Berko, A N Blacklocks et al.

[Glass polymorphism in amorphous germanium probed by first-principles computer simulations](#)

G Mancini, M Celino, F Iesari et al.

Data reduction for XAS experiments with the 100 element Ge Detector

L A Martín-Montoya^{1,2}, A Rothkirch¹ and W Caliebe¹

¹Deutsches Elektron Synchrotron (DESY), Notkestr. 85, 22607 Hamburg, Germany

²Universität Paderborn, Warburger Str. 100, 33098 Paderborn, Germany

E-mail: ligia.andrea.martin.montoya@desy.de

Abstract. X-ray absorption spectroscopy on dilute samples is still a challenge nowadays. By means of the fluorescence processes that follow the absorption it is possible to obtain the XAS spectrum; however, in order to gain sufficient statistics a multi-pixel fluorescence detector is required. A 100 pixel Ge detector will be available at beamline P64 at PETRA III for ultra dilute sample systems. Here, we propose a method of data reduction that resolves the line of interest from the scattering peak, improving the signal-to-noise ratio of the final XAS spectrum compared with the one obtained with a simple region of interest (ROI).

1. Introduction

Chemical processes on biological samples, like metalloproteins, are of great interest. X-ray Absorption Spectroscopy (XAS) allows to get structural and chemical information and does not require crystallinity; therefore, it is potentially an adequate tool for the investigation of disordered materials like metalloproteins in solution [1]. Those samples are typically in ultra dilute concentrations, meaning that the absorption is too low to be detected with the standard XAS in transmission mode [2]. This drawback can be overcome by measuring XAS in fluorescence mode and employing a multi-pixel fluorescence detector to improve the signal-to-noise ratio by a factor of \sqrt{n} , where n is the number of pixels [3, 4].

The beamline P64 at PETRA III is planned for BioXAS experiments among others. Those studies will be possible with the 100 pixel Germanium detector, that is a segmented-pixelated planar fluorescence detector where each pixel performs like a single detector, aiming to improve the signal-to-noise ratio of the final XAS spectrum by a factor of 10 [5]. The data collection works as follows: a full fluorescence spectrum is collected at a determined incident energy and per pixel, leading to a final 3D data array of dimensions $n \times k \times m$, where k is the number of incident beam energies and m is the length of each fluorescence spectra (see Figure 1). The 3D data array is to be reduced efficiently into a final XAS spectrum of length k .

2. Data Reduction

Reducing n fluorescence spectra at a single incident energy could be done in principle with an average. Nevertheless, this approach is not completely accurate since there can be several artifacts coming from some pixels that should not be taken into account e.g. glitches [6]. In



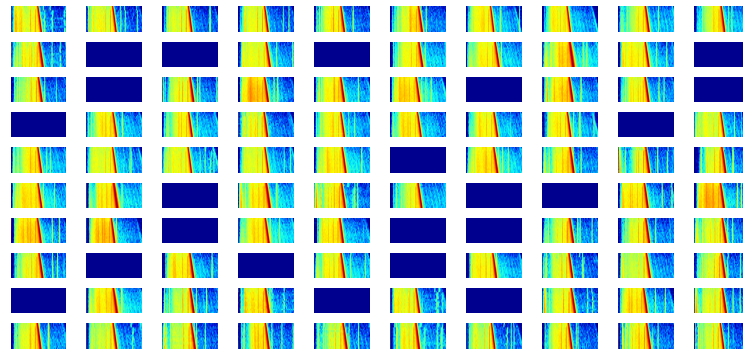


Figure 1. 3D data array of the sample $[\text{Cu}_2(\text{RSSR})_2](\text{OTf})_2$ measured at PETRA III P11. The image contains 100 pixels with incident energy vs. fluorescence energy where 78 pixels were turned on.

order to reject those pixels with low performance, we propose a method that at a single incident energy calculates a quantity Diff_i for each pixel i , as:

$$\text{Diff}_i = \hat{S}^j - S_i^j \quad (1)$$

where \hat{S}^j is the entry j of the mean fluorescence spectrum and S_i^j is the entry j of the fluorescence spectrum of the pixel i .

Only if Diff_i is equal or lower than the shot noise $\sqrt{\hat{S}^j}$ [4], it is taken into account for the final fluorescence spectrum. From this procedure 20 pixels were deleted from the mean. As an alternative, the median can be used instead of the mean spectrum in order to delete artifacts like glitches. A comparison between the three methods is exhibited in Figure 2 and shows that the corrected mean and the median decrease slightly the overlapping between the line of interest and the scattering.

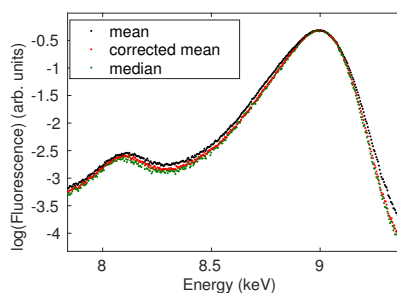


Figure 2. Comparison between the mean spectrum, the corrected mean without 20 rejected pixels and the median spectrum at the incident energy of 8.98 keV.

Since the position of the Compton scattering exposes an angular dependence and its intensity is comparable to the Thomson scattering at angles close to $\pi/2$, the width of the scattering line (Compton + Thomson) is different depending on the pixel's column at energies near the Cu absorption edge. Therefore, for accurateness the spectra should be analyzed by columns instead of an overall treatment of all the pixels.

Once the final fluorescence spectrum per incident energy is obtained, it is necessary to extract

the total number of counts under the fluorescence peak of interest. This value per incident energy would build up the final XAS spectrum. One of the procedures is made by a selection of a region of interest ROI around the peak of interest and a further integration of the number of counts in this region. However, the strong overlapping of the line of interest and the tail of the scattering line at energies close to the absorption edge makes this method inaccurate [7] (see Figure 3).

Aiming to extract the number of counts that correspond to the fluorescence line of interest, an automatic fitting procedure of a region between the line of interest and the scattering line is proposed. The line of interest as well as every fluorescence line in this region is fitted as a Gaussian function and the scattering line as an Exponentially Modified Gaussian Function *EMG* [8, 9, 10], described as:

$$EMG = A \exp \left[\frac{1}{2} \left(\frac{\sigma}{t_0} \right)^2 + \frac{x - \beta}{t_0} \right] \left[\operatorname{erf} \left(\frac{1}{2} \left[\frac{\beta}{\sigma} + \frac{\sigma}{t_0} \right] \right) + \operatorname{erf} \left(-\frac{x - \beta}{\sqrt{2}\sigma} - \frac{\sigma}{\sqrt{2}t_0} \right) \right], \quad (2)$$

where A is the amplitude, β the center, σ the FWHM and t_0 the skewness. This model allows to fit the strong asymmetry of the scattering line by means of the parameter t_0 .

The data from the sample $[\text{Cu}_2(\text{RSSR})_2](\text{OTf})_2$ measured at PETRA III beamline P11 was evaluated with the proposed fitting algorithm. At low energies (XANES) the fit includes a Gaussian, corresponding to CuK_α , plus an EMG (Figure 3).

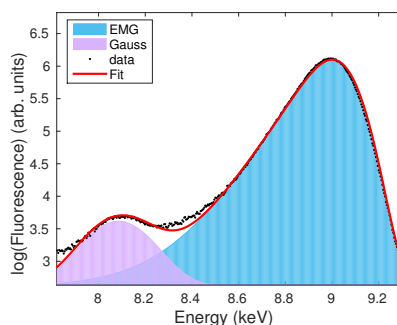


Figure 3. Data and fit result at an incident energy of 9 keV. Magenta denotes the Gaussian fit to the CuK_α line and blue the EMG fit to the scattering line. The final fit is indicated by the red curve.

The fitting algorithm was automatized to fit the amplitude of the Gaussian A_{gauss} correspondent to the CuK_α line at each incident energy and to determine the area under the Gaussian ($\sqrt{2\pi}A_{\text{gauss}}\sigma_{\text{gauss}}$) in order to build up the XANES spectrum (see Figure 4). To avoid as much as possible errors in the fitting procedure only the amplitudes of the Gaussians were fitted and other parameters were calculated based on the peak positions, typical skewness and FWHM. The fitting algorithm results in a smoother XAS curve compared to the ROI curve and the quality of the fit is always above the $R^2 = 0.998$.

The data under analysis corresponds to the first test beamtime of the 100 pixel Ge detector; therefore, due to set-up issues, it is too noisy to be analyzed as normal XAFS. Nevertheless, the XANES region on Figure 4 shows that the fitting algorithm gives a smoother curve than the ROI. Furthermore, the pre-edge region of the ROI curve is strongly contaminated by the scattering as shown in Figure 4. In this sense, the fitting algorithm is more reliable in the pre-edge and the XANES regions.

At higher energies, e.g. at the Mo absorption edge, the elastic and inelastic scattering peaks are discerned. In such a case, the data reduction should include a model that treats the Thomson and Compton lines independently.

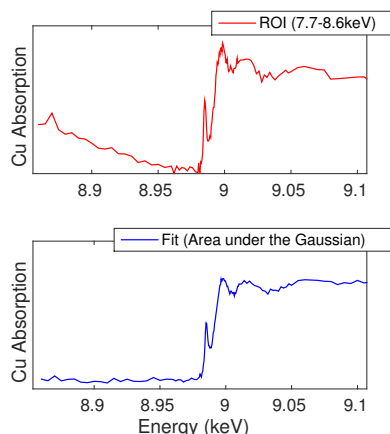


Figure 4. Final XANES spectra obtained by integration over a ROI between 7.7–8.6 keV (in red) and with the Area under the Gaussian, calculated with the proposed fitting algorithm (in blue).

3. Conclusions

Here we present an automatic routine of data reduction for the 100 pixel Ge detector with XAS experiments. The routine reduces 100 fluorescence spectra at each incident energy into one, by comparing each spectra to the average and dismissing those which difference is above the shot noise. A further fitting procedure that takes into account the asymmetry of the scattering peak is presented and compared to the ROI procedure to extract the XANES curve. The fitting algorithm proposed here gives satisfactory results in terms of goodness (R^2) and signal-to-noise ratio. The pre-edge region is better described with the fitting algorithm because the contamination from the scattering is reduced compared to the ROI algorithm.

Acknowledgments

We would like to thank the staff from PETRA III beamline P11 for help during the beamtime, our colleagues R. Chernikov, A. Kalinko, V. Murzin, M. Naumova, M. Tolkiehn, B. Walz and E. Welter, as well as the professors G. Henkel and J. Lindner for valuable discussions and encouragement, and an unknown reviewer for enlightening thoughts concerning Compton scattering. This project is funded by DESY and the BMBF project “BioXAS at PETRA III”.

References

- [1] Shi W *et al* 2011 Characterization of metalloproteins by high-throughput X-ray absorption spectroscopy *Cold Spring Harbor Laboratory Press* **21** 898–907
- [2] Ascone I, Meyer-Klaucke W and Murphy L 2003 Experimental aspects of biological X-ray absorption spectroscopy *J. Synchrotron Rad.* **10** 16–22
- [3] Cramer S P, Tench O, Yocum M and George G N 1988 A 13-element Ge detector for fluorescence EXAFS *Nuclear Instruments and Methods in Physics Research A* **266** 586–91
- [4] Janesick J R 2007 *Photon Transfer: DN \rightarrow λ , Chapter 3: Photon Transfer Noise Sources* Bellingham, Washington 98227-0010 USA SPIE 21–8
- [5] Camberra Industries, High-purity Germanium (HPGe) Detectors
- [6] Korbas M, Fulla Marsa D and Meyer-Klaucke W 2006 KEMP: A program script for automated biological x-ray absorption spectroscopy data reduction *Review of Scientific Instruments* **77** 063105
- [7] Tamenori Y, Moritab M and Nakamura T 2011 Two-dimensional approach to fluorescence yield XANES measurement using a silicon drift detector *J. Synchrotron Rad.* **18** 747–52
- [8] Hangi D and Carr P W 1985 Errors in Exponentially Modified Gaussian Equations in the Literature *Anal. Chem.* **57** 2394–95
- [9] Walz B 2011 Untersuchung von Fremdatomen in kristallinen Materialien mit kinematischen stehenden Röntgenwellen *Deutsches Elektronen-Synchrotron* 52–6
- [10] Eggert T, Boslau O, Kemmer J, Pahlke A and Wiest F 2006 The spectral response of silicon X-ray detectors *Nuclear Instruments and Methods in Physics Research A* **568** 1–11